Surgical Neurology International

OPEN ACCESS

For entire Editorial Board visit : http://www.surgicalneurologyint.com

Editor: **James I. Ausman,** MD, PhD University of California, Los Angeles, CA, USA

Original Article

Os odontoideum in identical twins: Comparative gene expression analysis

David Straus, Shunbin Xu[1], Vincent C. Traynelis

Departments of Neurological Surgery, and [1]Pharmacology, Ophthalmology and Neurological Sciences, Rush University Medical Center, Chicago, IL, USA

E-mail: David Straus - David_Straus@rush.edu; Shunbin Xu - Shunbin_Xu@rush.edu; *Vincent C. Traynelis - Vincent_Traynelis@rush.edu
*Corresponding author

Received: 04 December 13 Accepted: 06 February 14 Published: 20 March 14

This article may be cited as:
Straus D, Xu S, Traynelis VC. Os odontoideum in identical twins: Comparative gene expression analysis. Surg Neurol Int 2014;5:37.
Available FREE in open access from: http://www.surgicalneurologyint.com/text.asp?2014/5/1/37/129259

Abstract

Background: Os odontoideum is a well identified anomaly of the craniovertebral junction. Since its initial description, there has been a continuous debate regarding the nature of its etiology: Whether congenital or traumatic. We sought to compare the gene expression profiles in patients with congenital os odontoideum, those with traumatic os odontoideum and controls.

Methods: We have evaluated a pair of identical twins both with os odontoideum. We identified two additional patients with and four subjects without os odontoideum. We analyzed the gene expression profiles in these patients using a custom TaqMan microarray and quantitative reverse transcriptase polymerase chain reaction (qRT-PCR). The relative gene expression profiles in the two identical twins, the two nontwin patients with os odontoideum and the controls were assessed.

Results: A total of 213 genes with significantly different expression between the twin os odontoideum patients and the subjects without os odontoideum were detected. CACNG6, PHEX, CACNAD3, IL2, FAS, TUFT1, KIT, TGFBR2, and IGF2 were expressed at levels greater than 100-fold more in the twins. There were six genes with significantly different expression profiles in the twins as compared with the nontwin os odontoideum patients: CMK4, ATF1, PLCG1, TAB1, E2F3, and ATF4. There were no statistically significant differences in gene expression in the four patients with os odontoideum and the subjects without. Trends, however, were noted in MMP8, KIT, HIF1A, CREB3, PWHAZ, TGFBR1, NFKB2, FGFR1, IPO8, STAT1, COL1A1, and BMP3.

Conclusions: Os odontoideum has multiple etiologies, both traumatic and congenital and perhaps some represent a combination of the two. This work has identified a number of genes that show increased expression in a pair of twins with congenital os odontoideum and also demonstrates trends in gene expression profiles between a larger group of os odontoideum patients and non-os patients. A number of these genes are related to bone morphogenesis and maintenance.

Key Words: Anomaly, cervical spine, craniovertebral junction, identical twins, os odontoideum

Access this article online

Website: www.surgicalneurologyint.com

DOI: 10.4103/2152-7806.129259

Quick Response Code:

INTRODUCTION

Os odontoideum is a well-defined anatomic anomaly consisting of a smooth ossicle of bone separated from a shortened odontoid process.[1] The incidence and prevalence of os odontoideum is unknown. This entity was first described in 1886 by Giacomini, which has been followed by numerous publications debating its etiology. Two theories—congenital and traumatic—dominate the discussion. A recent review by Arvin *et al.*[3] provides an excellent discussion of the regional embryology and anatomy as related to the pathogenesis of os odontoideum. The congenital hypothesis is founded on the principle that the os odontoideum is a segmental defect, which represents a failed fusion of the odontoid and C2 vertebral body.[8] Conversely, the traumatic hypothesis considers the os odontoideum an acquired pathology resulting from avascular necrosis following an odontoid fracture.[11] The congenital hypothesis is supported by reports of identical twins both with os odontoideum[18] and two separate communications of families with an autosomal dominant inheritance pattern of os odontoideum.[26,43] Support of the traumatic hypothesis comes from the observation of a pair of identical twins one with os and one without[40] and from 13 patients reported in the literature who had radiographic documentation of a normal odontoid and subsequently acquired os odontoideum after a trauma.[11-13,31,35,37,42,48] In this manuscript we describe the genetic features of two identical male twins both with os odontoideum, their family members, other patients with traumatic os odontoideum, and control patients without an os odontoideum.

MATERIALS AND METHODS

Patients and study design

IRB approval was obtained from Rush University Medical Center and informed consent was obtained from participants.

Two 20-year-old identical male twins were evaluated in the neurosurgery clinic at Rush University Medical Center. Neither twin had a significant history of trauma and both were active collegiate water-polo players. The clinical presentation was related to neck pain in one of the twins. Imaging revealed an os odontoideum. Flexion-extension imaging revealed an orthotopic os odontoideum with gross instability. Given this finding his brother underwent similar evaluation with comparable results. Preoperative cervical spine films are shown in Figures 1 and 2.

Two additional, unrelated patients with an os odontoideum were subsequently treated. The first was a 49-year-old female who had a prior history of occipitocervical fusion at an outside hospital. She initially presented with hardware failure, pseudoarthrosis, and a wound infection. She did have a remote history of significant head trauma. Imaging revealed an os odontoideum, a C2-3 Klippel–Feil anomaly and a kyphotic deformity [Figure 3]. She ultimately underwent revision of her occipitocervical fusion. The second nontwin os patient was a 53-year-old female with neck

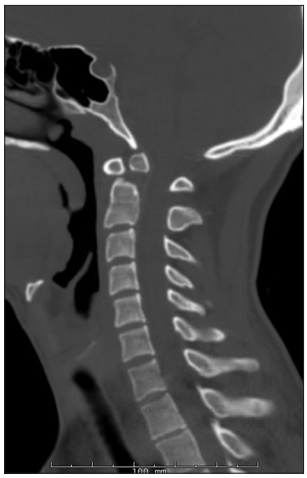

Figure 1: Preoperative sagittal cervical spine CT scan of Twin-1

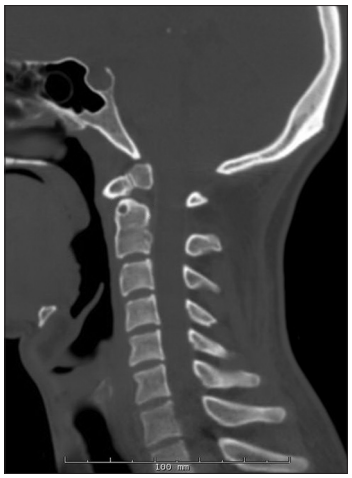

Figure 2: Preoperative sagittal cervical spine CT scan of Twin-2

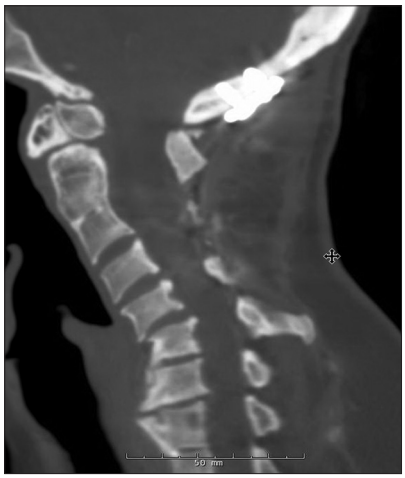

Figure 3: Preoperative sagittal cervical spine CT scan of non-twin Os-1

pain and myelopathy. Imaging studies revealed an unstable os odontoideum with cord compression at C1 [Figure 4]. She was treated with a C1-laminectomy and an instrumented atlanto-axial fusion.

Four subjects with prior cervical spine radiography that clearly demonstrated normal craniovertebral junction (CVJ) anatomy—absence of os odontoideum or other congenital anomaly—were identified to serve as controls. One of these subjects was the biological mother of the identical twins with os odontoideum. This control group included a 52-year-old female, an 87-year-old female, a 49-year-old male, and a 59-year-old female.

Comparisons were utilized in a case-control model and included relative gene expression levels between the identical twins with os odontoideum and the controls without os odontoideum; between the identical twins and the unrelated patients with os odontoideum; and finally, between all patients with os odontoideum and all controls without os odontoideum.

Sample collection and RNA preparation

Blood samples were collected via venipuncture from all patients into 5 ml collection tubes containing EDTA and immediately placed on ice. Total RNA from the blood cell pellet of each sample and isolated mRNA for gene expression profiling using the miRVana RNA isolation kit (Ambion, Grand Island, NY).

mRNA qRT-PCR array assays and data analysis

A total of 1 μg of RNA of each sample was used for gene expression profiling. Gene expression profiling was performed on the HT7900 real-time PCR system (Applied Biosystems, Foster City, CA) using custom TaqMan array cards (Applied Biosystems, Supplement 1) on all RNA samples. Reverse transcription was performed using the High Capacity cDNA Reverse Transcription Kit (Applied Biosystems) according to manufacturer's protocol. Amplification using the custom Taqman

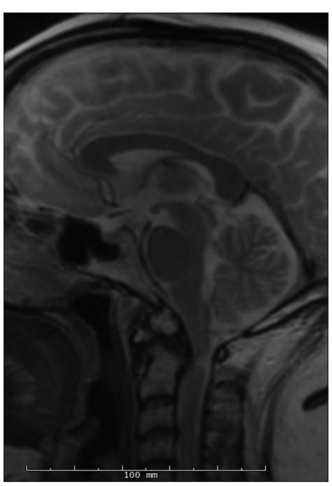

Figure 4: Preoperative sagittal T2-weighted cervical spine MRI of non-twin Os-2

Supplementary Table 1: Custom TaqMan Array design

18S-Hs99999901_s1 (endogenous control)	BAI1-Hs00181777_m1	CACNA1I-Hs00184168_m1	CAMK2D-Hs00241833_m1	CHEK2-Hs00200485_m1	CREBBP-Hs00231733_m1	ELK1-Hs00428286_g1	GJA5-Hs00979198_m1	GTF2B-Hs00155321_m1	IL2-Hs00174114_m1	MAPK1-Hs01046830_m1	PIAS1-Hs00184008_m1	PRKCA-Hs00176973_m1	RELB-Hs00232399_m1	SMAD7-Hs00178696_m1	TGFBR2-Hs00559661_m1
ABL1;BCR-Hs00245445_m1	BAX-Hs00180269_m1	CACNA1S-Hs00163885_m1	CAMK2G-Hs00538454_ m1	COL10A1-Hs00166657_m1	CREM-Hs01582003_g1	ENAM-Hs00230406_m1	GNAI1-Hs01053355_m1	GUSB-Hs99999908_m1	IL6-Hs00985639_m1	MAPK3-Hs00385075_m1	PIK3CA-Hs00180679_m1	PRKCB-Hs00176998_m1	REL-Hs00968436_m1	SMAD9-Hs00195441_m1	THBS1-Hs00962908_m1
ABL1-Hs01104728_m1	BCL2-Hs99999018_m1	CACNA2D1-Hs00167808_m1	CAMK4-Hs00174318_m1	COL11A1-Hs00266273_m1	CRP-Hs00357041_m1	EP300-Hs00230938_m1	GNAI2-Hs01064686_m1	HDAC10-Hs00368899_m1	INPP5D-Hs00183290_m1	MAPK8-Hs01548508_m1	PIK3CB-Hs00927728_m1	PRKCD-Hs01090047_m1	RPL30-Hs00265497_m1	SOS1-Hs00362308_m1	TNFRSF10B-Hs00366278_m1
ACTA1-Hs00559403_m1	BGLAP-Hs01587813_g1	CACNA2D2-Hs01021049_m1	CASC3-Hs00201226_m1	COL12A1-Hs00189184_m1	CSF2-Hs00171266_m1	FAS-Hs00531110_m1	GNAI3-Hs00197803_m1	HDAC11-Hs00227335_m1	IPO8-Hs00183533_m1	MAPK9-Hs00177102_m1	PIK3CD-Hs00192399_m1	PRKCE-Hs00178455_m1	RPL37A-Hs01102345_m1	SOST-Hs00228830_m1	TNFRSF11A-Hs00921374_m1
ACTB-Hs99999903_m1	BMP1-Hs00241807_m1	CACNA2D3-Hs01045030_m1	CASP10-Hs01017902_m1	COL14A1-Hs00385388_m1	CSF3-Hs99999083_m1	FGF1-Hs00265254_m1	GNAQ-Hs00387073_m1	HDAC1-Hs02621185_s1	ITPR1-Hs00181881_m1	MDM2-Hs99999008_m1	PIK3R1-Hs00381459_m1	PRKCG-Hs00177010_m1	RPLP0-Hs99999902_m1	SOX9-Hs00165814_m1	TNNT1-Hs00162848_m1
ACVR1-Hs00153836_m1	BMP2-Hs00154192_m1	CACNA2D4-Hs00297782_m1	CASP1-Hs00354836_m1	COL15A1-Hs00266332_m1	CSNK1D-Hs01017895_m1	FGF2-Hs00266645_m1	GNAS-Hs00255603_m1	HDAC2-Hs00231032_m1	ITPR2-Hs00181916_m1	MET-Hs00179845_m1	PIK3R2-Hs00178181_m1	PRKCZ-Hs00177051_m1	RPS17-Hs00734303_g1	SPARC-Hs00277762_m1	TP53-Hs01034249_m1
ACVR2B-Hs00609603_m1	BMP3-Hs00609638_m1	CACNB1-Hs00609501_m1	CASP2-Hs00234982_m1	COL16A1-Hs00156876_m1	DDR1-Hs00233612_m1	FGF3-Hs00173742_m1	GNB1-Hs00181845_m1	HDAC3-Hs00187320_m1	ITPR3-Hs00609908_m1	MGP-Hs00179899_m1	PLCB1-Hs00248563_m1	PRKDC-Hs00179161_m1	RUNX2-Hs00231692_m1	SPP1-Hs00959010_m1	TUFT1-Hs00360629_m1
ACVRL1-Hs00163543_m1	BMP4-Hs00370078_m1	CACNB2-Hs00167861_m1	CASP3-Hs00234387_m1	COL17A1-Hs00166711_m1	DMP1-Hs00189368_m1	FGFR1-Hs00241111_m1	GNB2-Hs00929275_g1	HDAC4-Hs00195814_m1	JMJD4-Hs01061169_m1	MINPP1-Hs00245149_m1	PLCB2-Hs00190117_m1	PSMA2-Hs00855061_sH	SATB1-Hs00161515_m1	STAT1-Hs01014002_m1	TWIST1-Hs00361186_m1
ADCY1-Hs00299832_m1	BMP5-Hs00234930_m1	CACNB3-Hs00167873_m1	CASP4-Hs01031947_m1	COL18A1-Hs00181017_m1	DSPP-Hs00171962_m1	FGFR2-Hs00240796_m1	GNB3-Hs01564092_m1	HDAC5-Hs00608366_m1	JUN-Hs99999141_s1	MMP13-Hs00233992_m1	PLCE1-Hs00275279_m1	PSMA3-Hs00541059_m1	SATB2-Hs00392652_m1	STAT3-Hs00374280_m1	TWIST2-Hs00382379_m1
ADCY3-Hs00269618_m1	BMP6-Hs00233470_m1	CACNB4-Hs00167878_m1	CASP5-Hs00237061_m1	COL19A1-Hs00156940_m1	DVL2-Hs00182901_m1	FGFR3-Hs00179829_m1	GNG2-Hs00828232_m1	HDAC6-Hs00195869_m1	KAT2B-Hs00187332_m1	MMP2-Hs00234422_m1	PLCG1-Hs00234046_m1	PSMA6-Hs00853240_sH	SFN-Hs00356613_m1	STATH-Hs00162389_m1	UBB-Hs00430290_m1
AHSG-Hs00155659_m1	BMP7-Hs00233476_m1	CACNG1-Hs00167887_m1	CASP6-Hs00154250_m1	COL1A1-Hs00164004_m1	E2F1-Hs00153451_m1	FLT1-Hs00176573_m1	GRB2-Hs00157817_m1	HDAC7-Hs00248789_m1	KDR-Hs00911700_m1	MMP8-Hs00233972_m1	PLCG2-Hs00182192_m1	PSMB2-Hs01002946_m1	SHH-Hs01123832_m1	TAB1-Hs00196143_m1	UBC-Hs00824723_m1
AKT1-Hs00178289_m1	BMP7-Hs00233477_m1	CACNG2-	CASP7-Hs00169152_m1	COL1A2-Hs00164099_m1	E2F2-Hs00231667_m1	FOS-Hs00170630_m1	GRIA1-Hs00181348_m1	HDAC8-Hs00218503_m1	KIT-Hs00174029_m1	MRPL19-Hs00608519_m1	POLR2A-Hs00172187_m1	PSMB4-Hs00160598_m1	SIRT1-Hs01009006_m1	TAB2-Hs00248373_m1	UBD-Hs00197374_m1
AKT2-Hs01086102_m1	BMPR1A-Hs00831730_s1	CACNG3-Hs00197985_m1	CASP8-Hs01018151_m1	COL2A1-Hs00264051_m1	E2F3-Hs00605457_m1	FOXH1-Hs00182690_m1	GRIA2-Hs00181331_m1	HDAC9-Hs00206843_m1	LTBP3-Hs00221445_m1	MSX1-Hs00427183_m1	POLR2B-Hs00265358_m1	PSMB5-Hs00605652_m1	SIRT2-Hs00247263_m1	TBP-Hs00427621_m1	VDR-Hs01045840_m1
AKT3-Hs00178533_m1	BMPR1A-Hs01034913_g1	CACNG4-Hs01061935_m1	CASP9-Hs00154260_m1	COL3A1-Hs00164103_m1	E2F4-Hs00608098_m1	GADD45A-Hs00169255_m1	GRIA3-Hs01557466_m1	HIF1A-Hs00936371_m1	MAP2K1-Hs00605615_mH	MSX2-Hs00751239_s1	POLR2C-Hs00160308_m1	PSMC2-Hs00739800_m1	SIRT3-Hs00202030_m1	TBP-Hs99999910_m1	VEGFA-Hs00900054_m1
ALPL-Hs00758162_m1	BMPR1B-Hs00176144_m1	CACNG5-Hs00274241_m1	CASR-Hs00173436_m1	COL4A3-Hs00184277_m1	E2F5-Hs00231092_m1	GADD45B-Hs00169587_m1	GRIA4-Hs00898778_m1	HIPK2-Hs00179759_m1	MAP2K2-Hs00360961_m1	MT-ATP6-Hs02596862_g1	POP4-Hs00198357_m1	PSMC3-Hs00267682_m1	SIRT4-Hs00202033_m1	TBX5-Hs01052563_m1	VEGFB-Hs00173634_m1
AMBN-Hs00212970_m1	BMPR2-Hs00176148_m1	CACNG6-Hs00230428_m1	CBFB-Hs00242387_m1	COL4A4-Hs00164150_m1	E2F6-Hs00242501_m1	GADD45G-Hs00198672_m1	GRIK2-Hs00222637_m1	HMBS-Hs00609297_m1	MAP2K3-Hs00177127_m1	NFKB1-Hs00765730_m1	POSTN-Hs01566748_m1	PSMC4-Hs00197826_m1	SIRT5-Hs00202043_m1	TCF4-Hs00162613_m1	VEGFC-Hs00153458_m1
AMELY-Hs00795181_m1	BRCA1-Hs01556193_m1	CACNG7-Hs00259061_m1	CCND1-Hs00765553_m1	COL4A5-Hs00166712_m1	EFNB1-Hs00270004_m1	GAPDH-Hs99999905_m1	GRM1-Hs00168250_m1	HOXA1-Hs00939046_m1	MAP2K4-Hs00387426_m1	NFKB2-Hs00174517_m1	PPIA-Hs99999904_m1	PSMC5-Hs00267687_m1	SIRT6-Hs00213036_m1	TFIP11-Hs00201749_m1	WNT1-Hs00180529_m1
ARSE-Hs00163677_m1	CACNA1B-Hs00609480_m1	CACNG8-Hs00375633_m1	CCNE1-Hs01026536_m1	COL5A1-Hs00609088_m1	EGF-Hs00153181_m1	GATA1-Hs01085823_m1	GRM2-Hs00356062_m1	HPRT1-Hs99999909_m1	MAP2K6-Hs00992389_m1	NKX2-5-Hs00231763_m1	PRKACA-Hs00427274_m1	PSMD4-Hs00356654_m1	SMAD1-Hs00195432_m1	TFRC-Hs99999911_m1	WNT2B-Hs00257131_m1
ATF1-Hs00270896_m1	CACNA1C-Hs00167681_m1	CALCR-Hs00156229_m1	CDH11-Hs00156438_m1	COL7A1-Hs00164310_m1	EGFR-Hs00193306_m1	GATA2-Hs00231119_m1	GRM3-Hs00936123_m1	HRAS-Hs00610483_m1	MAP3K7-Hs00177373_m1	OAZ1-Hs00427923_m1	PRKACB-Hs00176944_m1	PTEN-Hs01920652_s1	SMAD2-Hs00183425_m1	TGFB1-Hs00998133_m1	WNT2-Hs00608224_m1
ATF2-Hs00153179_m1	CACNA1D-Hs00167753_m1	CALM1-Hs00237233_m1	CDK2-Hs01548894_m1	COL9A2-Hs00156712_m1	EGFR-Hs01076078_m1	GATA3-Hs00231122_m1	GRM4-Hs00904641_m1	IBSP-Hs00173720_m1	MAPK10-Hs00373461_m1	PAX3-Hs00240950_m1	PRKACG-Hs01033925_s1	PTHLH-Hs00174969_m1	SMAD3-Hs00232222_m1	TGFB1-Hs99999918_m1	WNT3-Hs00229135_m1
ATF4-Hs00909568_g1	CACNA1E-Hs00167789_m1	CALM2-Hs00830212_s1	CDK4-Hs00175935_m1	COMP-Hs00164359_m1	EIF2B1-Hs00426752_m1	GATA4-Hs00171403_m1	GRM5-Hs00168275_m1	IGF1-Hs00153126_m1	MAPK11-Hs00177101_m1	PDGFA-Hs00234994_m1	PRKAR1A-Hs00267597_m1	PUM1-Hs00206469_m1	SMAD4-Hs00232068_m1	TGFB2-Hs00234244_m1	YWHAZ-Hs00237047_m1
ATM-Hs01112307_m1	CACNA1F-Hs00913730_m1	CALM3-Hs00270914_m1	CDKN1A-Hs00355782_m1	CREB1-Hs00231713_m1	EIF4E-Hs00908915_g1	GATA5-Hs00388359_m1	GRM7-Hs00356067_m1	IGF1R-Hs00609566_m1	MAPK12-Hs00268060_m1	PES1-Hs00362795_g1	PRKAR1B-Hs00406762_m1	RAF1-Hs00234119_m1	SMAD4-Hs00929647_m1	TGFB3-Hs00234245_m1	
ATR-Hs00354807_m1	CACNA1G-Hs00367969_m1	CAMK2A-Hs00211096_m1	CDKN1B-Hs00153277_m1	CREB3-Hs00197255_m1	ELF1-Hs00152844_m1	GATA6-Hs00232018_m1	GRM8-Hs00168299_m1	IGF2-Hs00171254_m1	MAPK13-Hs00234085_m1	PGK1-Hs99999906_m1	PRKAR2A-Hs00177760_m1	RB1-Hs01078066_m1	SMAD5-Hs00195437_m1	TGFBI-Hs00165908_m1	
B2M-Hs99999907_m1	CACNA1H-Hs01103523_m1	CAMK2B-Hs00365799_m1	CHEK1-Hs00967506_m1	CREB3L4-Hs00370116_m1	ELF4-Hs01086125_m1	GDF10-Hs00192033_m1	GSK3B-Hs00275656_m1	IHH-Hs00745531_s1	MAPK14-Hs00176247_m1	PHEX-Hs01011692_m1	PRKAR2B-Hs00176966_m1	RELA-Hs00153294_m1	SMAD6-Hs00178579_m1	TGFBR1-Hs00610319_m1	n=381

array cards was performed using the Taqman Gene Expression Master mix (Applied Biosystem) according to manufacturer's protocol on a 7900HTReal-time PCR system at the miRNA and Gene Expression Core, Rush University Medical Center. All card amplification reactions were successful. Amplification data were acquired using the SDS2.3/RQ Manager (Applied Biosystems) and DataAssist 3.01 software (Applied Biosystems). The relative expression level for each mRNA was represented as cycle threshold (Ct). mRNAs with Ct < 40 were accepted as "detected". Eukaryotic 18s rRNA (18S-Hs99999901_s1) was identified as the most stably expressed endogenous control was used as the normalization control. Normalized expression level was calculated as Delta CT (DCt) or ΔCt = Ct (test RNA) -Ct (18s RNA). Differential expression between patients was calculated as DDCt or Δ(ΔCt) = Ave DCt (test) - Ave DCt (control). Fold change or relative quantification (RQ) was calculated as $RQ = 2^{-\Delta(\Delta Ct)}$. The Benjamini–Hochberg method[5] was applied to minimize the false discovery rate. An adjusted $P < 0.05$ was set as the criterion for significance of differential expression. FiRe Macro[15] was used in Microsoft Excel (Microsoft Corporation, Redmond, WA) to generate heatmaps of the normalized RNA expression levels.

Functional analysis

To better understand the functions of the differentially expressed mRNAs, we performed a NCBI Gene search[28] using the test RNA as a key word to compile known functions of this mRNA. We report the NCBI Gene Summary of selected genes in Tables 1, 3, and 4.

RESULTS

A comparison between the identical twins with os odontoideum (Twins) to the four control subjects (non-os) revealed 213 statistically significant differences in gene expression. The top 30 genes and a brief summary[23,28] of their function are provided in Table 1. Nine genes were expressed in the Twins at levels greater-than 100 times that of the non-os group. CACNG6 showed a 565-fold increase in expression in the Twins ($P < 0.05$). This mRNA is derived from a gene located on chromosome 19p13.4 and encodes the gamma-6 subunit of the voltage dependant calcium channel. PHEX expression was 447-fold higher in the Twins ($P < 0.005$). The PHEX mRNA encodes a transmembrane zinc-dependent endopeptidase involved in bone and dentin mineralization and renal phosphate reabsorption. CACNA2D3 showed a 125-fold increase in the Twins ($P < 0.005$). This gene is located on chromosome 3p21.2 and encodes the alpha-2/delta-3 subunit in the voltage-dependent calcium channel. Interleukin 2 (IL2) was increased 116-fold in the Twins ($P < 0.0005$); this gene is located on 4q26-q27 and encodes an inflammatory cytokine that is important for T- and B-cell proliferation. FAS was increased 113-fold in the Twins ($P < 0.05$); this gene is located on chromosome 10q24.1 and encodes a transmembrane protein important in mediating the extrinsic pathway of apoptosis. It is also involved in transducing proliferative signals from normal fibroblasts and T-cells. TUFT1 was increased 109-fold ($P < 0.005$) in the Twins; this gene is located on chromosome 1q21 and is involved in the mineralization and structural organization of enamel. KIT was increased 107-fold in the Twins ($P < 0.0005$); this gene is located on 4q11-q12 and encodes a transmembrane receptor for mast cell growth factor. It is a proto-oncogene and mutations are associated with malignancies (e.g. gastrointestinal stromal tumor and acute myelogenous leukemia). TGFBR2 was increased 102-fold in the twins ($P < 0.05$). This gene is located on chromosome 3p22 and encodes a transmembrane Ser/Thr protein kinase related to cell proliferation. Mutations have been associated with Marfan syndrome, Loeys–Dietz Aortic Aneurysm Syndrome and various malignancies. IGF2 was increased 101-fold in the Twins ($P < 0.05$); this gene is located on 11p15.5 and encodes a member of the insulin-like growth factors that is a major fetal growth factor. Complete results of all 213 genes with significant differences in expression between the Twins and non-os groups are shown in Table 2.

Comparing the Twins with the two unrelated patients with os odontoideum (non-Twin os) revealed six genes with statistically significant differences in expression. These genes and a brief summary of their functions are presented in Table 3. CAMK4 was increased 31-fold in the Twins as compared with the non-Twin os patients ($P < 0.05$). This gene is located on chromosome 5q21.3 and encodes a calcium-calmodulin dependent Ser/Thr kinase. ATF1 was increased 23-fold in the Twins ($P < 0.05$); this gene is located on chromosome 12q13 and encodes an activating transcription factor and fusion products have been implicated in angiomatoid fibrous histiocytoma and clear cell sarcoma. Expression of PLCG1 was increased 21-fold in the Twins ($P < 0.05$). This gene encodes gamma-1 phospholipase-C and is located on chromosome 20q12-q13.1. TAB1 was increased 21-fold ($P < 0.05$); this gene is located on chromosome 22q13.1 and encodes a protein involved in the regulation of the MAP kinase pathway. E2F3 was increased 19-fold ($P < 0.05$). This gene is located on chromosome 6p22 and encodes a protein regulator of the cell cycle. ATF4 was found to be elevated 14-fold in the Twins ($P < 0.05$); this gene is located on chromosome 22q13.1 and encodes a transcription factor that modulates DNA transcription in response to cAMP.

Comparing both the Twins and non-Twin os (Os) to the non-os group revealed no statistically significant differences in gene expression. We report the 10 genes with the greatest fold-change and an unadjusted $P < 0.1$ [Table 4].

Table 1: Top 30 gene expression differences between Twins and non-os

Twin os ($n=2$) vs non-os ($n=4$)				
Gene	**R/Q**	**BH**	**Location**	**NCBI Gene summary[28]**
CACNG6	565.44	$P<0.05$	19q13.4	Voltage-dependent calcium channels are composed of five subunits. The protein encoded by this gene represents one of these subunits, gamma, and is one of two known gamma subunit proteins. This particular gamma subunit is an integral membrane protein that is thought to stabilize the calcium channel in an inactive (closed) state. This gene is part of a functionally diverse eight-member protein subfamily of the PMP-22/EMP/MP20 family and is located in a cluster with two family members that function as transmembrane AMPA receptor regulatory proteins (TARPs). Alternative splicing results in multiple transcript variants. Variants in this gene have been associated with aspirin-intolerant asthma
PHEX	446.70	$P<0.005$	Xp22.2-p22.1	The protein encoded by this gene is a transmembrane endopeptidase that belongs to the type II integral membrane zinc-dependent endopeptidase family. The protein is thought to be involved in bone and dentin mineralization and renal phosphate reabsorption. Mutations in this gene cause X-linked hypophosphatemic rickets
CACNA2D3	124.92	$P<0.005$	3p21.1	This gene encodes a member of the alpha-2/delta subunit family, a protein in the voltage-dependent calcium channel complex. Calcium channels mediate the influx of calcium ions into the cell upon membrane polarization and consist of a complex of alpha-1, alpha-2/delta, beta, and gamma subunits in a 1:1:1:1 ratio. Various versions of each of these subunits exist, either expressed from similar genes or the result of alternative splicing. Research on a highly similar protein in rabbit suggests the protein described in this record is cleaved into alpha-2 and delta subunits. Alternate transcriptional splice variants of this gene have been observed but have not been thoroughly characterized
IL2	116.28	$P<0.0005$	4q26-q27	The protein encoded by this gene is a secreted cytokine that is important for the proliferation of T and B lymphocytes. The receptor of this cytokine is a heterotrimeric protein complex whose gamma chain is also shared by interleukin 4 (IL4) and IL7. The expression of this gene in mature thymocytes is monoallelic, which represents an unusual regulatory mode for controlling the precise expression of a single gene. The targeted disruption of a similar gene in mice leads to ulcerative colitis-like disease, which suggests an essential role of this gene in the immune response to antigenic stimuli
FAS	113.27	$P<0.05$	10q24.1	The protein encoded by this gene is a member of the TNF-receptor superfamily. This receptor contains a death domain. It has been shown to play a central role in the physiological regulation of programmed cell death, and has been implicated in the pathogenesis of various malignancies and diseases of the immune system. The interaction of this receptor with its ligand allows the formation of a death-inducing signaling complex that includes Fas-associated death domain protein (FADD), caspase 8, and caspase 10. The autoproteolytic processing of the caspases in the complex triggers a downstream caspase cascade, and leads to apoptosis. This receptor has been also shown to activate NF-kB, MAPK3/ERK1, and MAPK8/JNK, and is found to be involved in transducing the proliferating signals in normal diploid fibroblast and T cells. Several alternatively spliced transcript variants have been described, some of which are candidates for nonsense-mediated mRNA decay (NMD). The isoforms lacking the transmembrane domain may negatively regulate the apoptosis mediated by the full length isoform
TUFT1	108.81	$P<0.005$	1q21	Involved in the mineralization and structural organization of enamel
KIT	107.28	$P<0.0005$	4q11-q12	This gene encodes the human homolog of the proto-oncogene c-kit. C-kit was first identified as the cellular homolog of the feline sarcoma viral oncogene v-kit. This protein is a type 3 transmembrane receptor for MGF (mast cell growth factor, also known as stem cell factor). Mutations in this gene are associated with gastrointestinal stromal tumors, mast cell disease, acute myelogenous leukemia, and piebaldism. Multiple transcript variants encoding different isoforms have been found for this gene
TGFBR2	102.40	$P<0.05$	3p22	This gene encodes a member of the Ser/Thr protein kinase family and the TGFB receptor subfamily. The encoded protein is a transmembrane protein that has a protein kinase domain, forms a heterodimeric complex with another receptor protein, and binds TGF-beta. This receptor/ligand complex phosphorylates proteins, which then enter the nucleus and regulate the transcription of a subset of genes related to cell proliferation. Mutations in this gene have been associated with Marfan Syndrome, Loeys-Dietz Aortic Aneurysm Syndrome, and the development of various types of tumors. Alternatively spliced transcript variants encoding different isoforms have been characterized

(*Contd*...)

Table 1: Continued

Twin os (n=2) vs non-os (n=4)				
Gene	**R/Q**	**BH**	**Location**	**NCBI Gene summary[28]**
IGF2	101.36	$P<0.05$	11p15.5	This gene encodes a member of the insulin family of polypeptide growth factors, which are involved in development and growth. It is an imprinted gene, expressed only from the paternal allele, and epigenetic changes at this locus are associated with Wilms tumor, Beckwith–Wiedemann syndrome, rhabdomyosarcoma, and Silver–Russell syndrome. A read-through INS-IGF2 gene exists, whose 5′ region overlaps the INS gene and the 3′ region overlaps this gene. Alternatively spliced transcript variants encoding different isoforms have been found for this gene
PLCG2	99.79	$P<0.005$	16q24.1	The protein encoded by this gene is a transmembrane signaling enzyme that catalyzes the conversion of 1-phosphatidyl-1D-myo-inositol 4,5-bisphosphate to 1D-myo-inositol 1,4,5-trisphosphate (IP3) and DAG, using calcium as a cofactor. IP3 and DAG are second messenger molecules important for transmitting signals from growth factor receptors and immune system receptors across the cell membrane
CACNA1H	97.34	$P<0.05$	16p13.3	This gene encodes a T-type member of the alpha-1 subunit family, a protein in the voltage-dependent calcium channel complex. Calcium channels mediate the influx of calcium ions into the cell upon membrane polarization and consist of a complex of alpha-1, alpha-2/delta, beta, and gamma subunits in a 1:1:1:1 ratio. The alpha-1 subunit has 24 transmembrane segments and forms the pore through which ions pass into the cell. There are multiple isoforms of each of the proteins in the complex, either encoded by different genes or the result of alternative splicing of transcripts. Alternate transcriptional splice variants, encoding different isoforms, have been characterized for the gene described here. Studies suggest certain mutations in this gene lead to childhood absence epilepsy (CAE)
TGFBI	91.58	$P<0.05$	5q31	This gene encodes an RGD-containing protein that binds to type I, II and IV collagens. The RGD motif is found in many extracellular matrix proteins modulating cell adhesion and serves as a ligand recognition sequence for several integrins. This protein plays a role in cell–collagen interactions and may be involved in endochondral bone formation in cartilage. The protein is induced by transforming growth factor-beta and acts to inhibit cell adhesion. Mutations in this gene are associated with multiple types of corneal dystrophy
MMP8	90.29	$P<0.0001$	11q22.3	Proteins of the matrix metalloproteinase (MMP) family are involved in the breakdown of extracellular matrix in normal physiological processes, such as embryonic development, reproduction, and tissue remodeling, as well as in disease processes, such as arthritis and metastasis. Most MMPs are secreted as inactive proproteins, which are activated when cleaved by extracellular proteinases. However, the enzyme encoded by this gene is stored in secondary granules within neutrophils and is activated by autolytic cleavage. Its function is degradation of type I, II and III collagens. The gene is part of a cluster of MMP genes, which localize to chromosome 11q22.3
CACNA2D2	86.02	$P<0.05$	3p21.3	This gene encodes a member of the alpha-2/delta subunit family, a protein in the voltage-dependent calcium channel complex. Calcium channels mediate the influx of calcium ions into the cell upon membrane polarization and consist of a complex of alpha-1, alpha-2/delta, beta, and gamma subunits in a 1:1:1:1 ratio. Various versions of each of these subunits exist, either expressed from similar genes or the result of alternative splicing. Research on a highly similar protein in rabbit suggests the protein described in this record is cleaved into alpha-2 and delta subunits. Alternate transcriptional splice variants of this gene, encoding different isoforms, have been characterized
SMAD7	83.99	$P<0.05$	18q21.1	The protein encoded by this gene is a nuclear protein that binds the E3 ubiquitin ligase SMURF2. Upon binding, this complex translocates to the cytoplasm, where it interacts with TGF-beta receptor type-1 (TGFBR1), leading to the degradation of both the encoded protein and TGFBR1. Expression of this gene is induced by TGFBR1. Variations in this gene are a cause of susceptibility to colorectal cancer type 3 (CRCS3). Several transcript variants encoding different isoforms have been found for this gene
TBP	77.39	$P<0.005$	6q27	Initiation of transcription by RNA polymerase II requires the activities of more than 70 polypeptides. The protein that coordinates these activities is transcription factor IID, which binds to the core promoter to position the polymerase properly, serves as the scaffold for assembly of the remainder of the transcription complex, and acts as a channel for regulatory signals. TFIID is composed of the TATA-binding protein and a group of evolutionarily conserved proteins known as TBP-associated factors or TAFs. TAFs may participate in basal transcription, serve as coactivators, function in promoter recognition or modify general transcription factors (GTFs) to

(*Contd*...)

Table 1: Continued

Twin os (n=2) vs non-os (n=4)				
Gene	**R/Q**	**BH**	**Location**	**NCBI Gene summary[28]**
				facilitate complex assembly and transcription initiation. This gene encodes TBP. A distinctive feature of TBP is a long string of glutamines in the N-terminus. This region of the protein modulates the DNA binding activity of the C terminus, and modulation of DNA binding affects the rate of transcription complex formation and initiation of transcription. The number of CAG repeats encoding the polyglutamine tract is usually 32-39, and expansion of the number of repeats increases the length of the polyglutamine string and is associated with spinocerebellar ataxia 17, a neurodegenerative disorder classified as a polyglutamine disease. Two transcript variants encoding different isoforms have been found for this gene
UBC	77.01	$P<0.05$	12q24.3	This gene represents an ubiquitin gene, ubiquitin C. The encoded protein is a polyubiquitin precursor. Conjugation of ubiquitin monomers or polymers can lead to various effects within a cell, depending on the residues to which ubiquitin is conjugated. Ubiquitination has been associated with protein degradation, DNA repair, cell cycle regulation, kinase modification, endocytosis, and regulation of other cell signaling pathways
NFKB1	76.42	$P<0.05$	4q24	This gene encodes a 105 kDa protein, which can undergo cotranslational processing by the 26S proteasome to produce a 50 kDa protein. The 105 kDa protein is a Rel protein-specific transcription inhibitor and the 50 kDa protein is a DNA binding subunit of the NF-kappa-B (NFKB) protein complex. NFKB is a transcription regulator that is activated by various intra- and extra-cellular stimuli such as cytokines, oxidant-free radicals, ultraviolet irradiation, and bacterial or viral products. Activated NFKB translocates into the nucleus and stimulates the expression of genes involved in a wide variety of biological functions. Inappropriate activation of NFKB has been associated with a number of inflammatory diseases while persistent inhibition of NFKB leads to inappropriate immune cell development or delayed cell growth. Two transcript variants encoding different isoforms have been found for this gene
PLCB2	74.99	$P<0.0005$	15q15	The protein encoded by this gene is a transmembrane signaling enzyme that catalyzes the conversion of 1-phosphatidyl-1D-myo-inositol 4,5-bisphosphate to 1D-myo-inositol 1,4,5-trisphosphate (IP3) and diacylglycerol (DAG), using calcium as a cofactor. IP3 and DAG are second messenger molecules important for transmitting signals from growth factor receptors and immune system receptors across the cell membrane
GATA2	72.84	$P<0.005$	3q21.3	This gene encodes a member of the GATA family of zinc-finger transcription factors that are named for the consensus nucleotide sequence they bind in the promoter regions of target genes. The encoded protein plays an essential role in regulating transcription of genes involved in the development and proliferation of hematopoietic and endocrine cell lineages. Alternative splicing results in multiple transcript variants
SIRT6	72.37	$P<0.005$	19p13.3	This gene encodes a member of the sirtuin family of proteins, homologs to the yeast Sir2 protein. Members of the sirtuin family are characterized by a sirtuin core domain and grouped into four classes. The functions of human sirtuins have not yet been determined; however, yeast sirtuin proteins are known to regulate epigenetic gene silencing and suppress recombination of rDNA. Studies suggest that the human sirtuins may function as intracellular regulatory proteins with mono-ADP-ribosyltransferase activity. The protein encoded by this gene is included in class IV of the sirtuin family. Alternative splicing results in multiple transcript variants
TBP	71.91	$P<0.005$	6q27	Initiation of transcription by RNA polymerase II requires the activities of more than 70 polypeptides. The protein that coordinates these activities is TFIID, which binds to the core promoter to position the polymerase properly, serves as the scaffold for assembly of the remainder of the transcription complex, and acts as a channel for regulatory signals. TFIID is composed of the TBP and a group of evolutionarily conserved proteins known as TBP-associated factors or TAFs. TAFs may participate in basal transcription, serve as coactivators, function in promoter recognition or modify GTFs to facilitate complex assembly and transcription initiation. This gene encodes TBP. A distinctive feature of TBP is a long string of glutamines in the N-terminus. This region of the protein modulates the DNA binding activity of the C terminus, and modulation of DNA binding affects the rate of transcription complex formation and initiation of transcription. The number of CAG repeats encoding the polyglutamine tract is usually 32-39, and expansion of the number of repeats increases the length of the polyglutamine string and is associated with spinocerebellar ataxia 17, a neurodegenerative disorder classified as a polyglutamine disease. Two transcript variants encoding different isoforms have been found for this gene

(*Contd*...)

Table 1: Continued

Twin os ($n=2$) vs non-os ($n=4$)				
Gene	**R/Q**	**BH**	**Location**	**NCBI Gene summary[28]**
PRKCZ	71.11	$P<0.05$	1p36.33-p36.2	Protein kinase C (PKC) zeta is a member of the PKC family of serine/threonine kinases, which are involved in a variety of cellular processes such as proliferation, differentiation and secretion. Unlike the classical PKC isoenzymes, which are calcium-dependent, PKC zeta exhibits a kinase activity, which is independent of calcium and diacylglycerol but not of phosphatidylserine. Furthermore, it is insensitive to typical PKC inhibitors and cannot be activated by phorbol ester. Unlike the classical PKC isoenzymes, it has only a single zinc finger module. These structural and biochemical properties indicate that the zeta subspecies is related to, but distinct from other isoenzymes of PKC. Alternative splicing results in multiple transcript variants encoding different isoforms
CREB3	69.57	$P<0.005$	9p13.3	This gene encodes a transcription factor that is a member of the leucine zipper family of DNA binding proteins. This protein binds to the cAMP-response element and regulates cell proliferation. The protein interacts with host cell factor C1, which also associates with the herpes simplex virus (HSV) protein VP16 that induces transcription of HSV immediate-early genes. This protein and VP16 both bind to the same site on host cell factor C1. It is thought that the interaction between this protein and host cell factor C1 plays a role in the establishment of latency during HSV infection. This protein also plays a role in leukocyte migration, tumor suppression, and endoplasmic reticulum stress-associated protein degradation. Additional transcript variants have been identified, but their biological validity has not been determined
CAMK4	67.76	$P<0.0001$	5q21.3	The product of this gene belongs to the serine/threonine protein kinase family, and to the Ca (2+)/calmodulin-dependent protein kinase subfamily. This enzyme is a multifunctional serine/threonine protein kinase with limited tissue distribution, which has been implicated in transcriptional regulation in lymphocytes, neurons, and male germ cells
CASP4	67.28	$P<0.0005$	11q22.2-q22.3	This gene encodes a protein that is a member of the cysteine-aspartic acid protease (caspase) family. Sequential activation of caspases plays a central role in the execution-phase of cell apoptosis. Caspases exist as inactive proenzymes composed of a prodomain and a large and small protease subunit. Activation of caspases requires proteolytic processing at conserved internal aspartic residues to generate a heterodimeric enzyme consisting of the large and small subunits. This caspase is able to cleave and activate its own precursor protein, as well as caspase 1 precursor. When overexpressed, this gene induces cell apoptosis. Alternative splicing results in transcript variants encoding distinct isoforms
YWHAZ	67.13	$P<0.005$	8q23.1	This gene product belongs to the 14-3-3 family of proteins, which mediate signal transduction by binding to phosphoserine-containing proteins. This highly conserved protein family is found in both plants and mammals, and this protein is 99% identical to the mouse, rat and sheep orthologs. The encoded protein interacts with IRS1 protein, suggesting a role in regulating insulin sensitivity. Several transcript variants that differ in the 5′ UTR but that encode the same protein have been identified for this gene
POLR2C	66.64	$P<0.05$	16q13-q21	This gene encodes the third largest subunit of RNA polymerase II, the polymerase responsible for synthesizing messenger RNA in eukaryotes. The product of this gene contains a cysteine rich region and exists as a heterodimer with another polymerase subunit, POLR2J. These two subunits form a core subassembly unit of the polymerase. A pseudogene has been identified on chromosome 21
RUNX2	66.00	$P<0.005$	6p21	This gene is a member of the RUNX family of transcription factors and encodes a nuclear protein with a Runt DNA-binding domain. This protein is essential for osteoblastic differentiation and skeletal morphogenesis and acts as a scaffold for nucleic acids and regulatory factors involved in skeletal gene expression. The protein can bind DNA both as a monomer or, with more affinity, as a subunit of a heterodimeric complex. Mutations in this gene have been associated with the bone development disorder cleidocranial dysplasia. Transcript variants that encode different protein isoforms result from the use of alternate promoters as well as alternate splicing
E2F3	65.11	$P<0.0001$	6p22	The protein encoded by this gene is a member of the E2F family of transcription factors. The E2F family plays a crucial role in the control of cell cycle and action of tumor suppressor proteins and is also a target of the transforming proteins of small DNA tumor viruses. The E2F proteins contain several evolutionally conserved domains found in most members of the family. These domains include a DNA binding domain, a dimerization domain, which determines interaction with the differentiation regulated transcription factor proteins (DP), a transactivation domain enriched in acidic amino acids, and a tumor suppressor protein association domain, which is embedded within the transactivation domain. This protein and another 2 members, E2F1 and E2F2, have an additional cyclin binding domain. This protein binds specifically to retinoblastoma protein pRB in a cell-cycle dependent manner. Two transcript variants encoding different isoforms have been found for this gene

TFIID: Transcription factor IID, TBP: TATA-binding protein, BH: Benjamini-Hochberg correction, RQ: Relative quantification value

Table 2: Complete results of os vs. non-os relative gene expression

Twin os (n=2) vs non-os (n=4)		
Gene	**R/Q**	**BH (56%)**
CACNG6-Hs00230428_m1	565.442076	$P<0.05$
PHEX-Hs01011692_m1	446.7033746	$P<0.005$
CACNA2D3-Hs01045030_m1	124.9153678	$P<0.005$
IL2-Hs00174114_m1	116.2778264	$P<0.0005$
FAS-Hs00531110_m1	113.2674924	$P<0.05$
TUFT1-Hs00360629_m1	108.8061243	$P<0.005$
KIT-Hs00174029_m1	107.2826289	$P<0.0005$
TGFBR2-Hs00559661_m1	102.401766	$P<0.05$
IGF2-Hs00171254_m1	101.3615162	$P<0.05$
PLCG2-Hs00182192_m1	99.78758191	$P<0.005$
CACNA1H-Hs01103523_m1	97.34123004	$P<0.05$
TGFBI-Hs00165908_m1	91.5777402	$P<0.05$
MMP8-Hs00233972_m1	90.29371725	$P<0.0001$
CACNA2D2-Hs01021049_m1	86.02436482	$P<0.05$
SMAD7-Hs00178696_m1	83.99117987	$P<0.05$
TBP-Hs99999910_m1	77.38842737	$P<0.005$
UBC-Hs00824723_m1	77.01042068	$P<0.05$
NFKB1-Hs00765730_m1	76.42075734	$P<0.05$
PLCB2-Hs00190117_m1	74.9898958	$P<0.0005$
GATA2-Hs00231119_m1	72.83520954	$P<0.005$
SIRT6-Hs00213036_m1	72.36975003	$P<0.005$
TBP-Hs00427621_m1	71.90909955	$P<0.005$
PRKCZ-Hs00177051_m1	71.10906373	$P<0.05$
CREB3-Hs00197255_m1	69.57215719	$P<0.005$
CAMK4-Hs00174318_m1	67.7555896	$P<0.0001$
CASP4-Hs01031947_m1	67.27551	$P<0.0005$
YWHAZ-Hs00237047_m1	67.1263045	$P<0.005$
POLR2C-Hs00160308_m1	66.63915512	$P<0.05$
RUNX2-Hs00231692_m1	65.995599	$P<0.005$
E2F3-Hs00605457_m1	65.10544495	$P<0.0001$
SMAD5-Hs00195437_m1	61.96846685	$P<0.05$
ELF4-Hs01086125_m1	61.74899285	$P<0.005$
GNAI3-Hs00197803_m1	61.3856538	$P<0.05$
PSMA3-Hs00541059_m1	59.90719904	$P<0.005$
RELA-Hs00153294_m1	58.51434644	$P<0.005$
CSNK1D-Hs01017895_m1	57.87562737	$P<0.005$
GNAI2-Hs01064686_m1	57.49499065	$P<0.005$
TGFBR1-Hs00610319_m1	57.37234408	$P<0.005$
GNG2-Hs00828232_m1	56.75024144	$P<0.005$
POLR2B-Hs00265358_m1	54.65071194	$P<0.05$
PIK3CD-Hs00192399_m1	54.15796684	$P<0.005$
GNAQ-Hs00387073_m1	53.36054444	$P<0.005$
SIRT5-Hs00202043_m1	52.99381137	$P<0.005$
E2F5-Hs00231092_m1	52.51367852	$P<0.005$
GADD45B-Hs00169587_m1	52.407263	$P<0.05$
CASP7-Hs00169152_m1	51.68136143	$P<0.005$
MRPL19-Hs00608519_m1	50.97490762	$P<0.0005$
TCF4-Hs00162613_m1	50.25789151	$P<0.005$
NFKB2-Hs00174517_m1	48.7725478	$P<0.005$
VEGFA-Hs00900054_m1	48.4581505	$P<0.05$
CREBBP-Hs00231733_m1	47.78444394	$P<0.005$
CASP8-Hs01018151_m1	46.28991997	$P<0.05$
FGFR1-Hs00241111_m1	46.06621367	$P<0.0005$
PRKAR1A-Hs00267597_m1	45.75140814	$P<0.05$
MAPK9-Hs00177102_m1	45.27242174	$P<0.005$
IPO8-Hs00183533_m1	44.70904295	$P<0.005$
IGF1R-Hs00609566_m1	44.33924933	$P<0.05$
REL-Hs00968436_m1	44.31068845	$P<0.0005$
PLCG1-Hs00234046_m1	44.1343681	$P<0.0005$
SOS1-Hs00362308_m1	43.58778631	$P<0.05$
MAPK13-Hs00234085_m1	43.51318621	$P<0.005$
STAT1-Hs01014002_m1	43.15939505	$P<0.05$
TFIP11-Hs00201749_m1	43.00329653	$P<0.005$
AKT1-Hs00178289_m1	42.35735581	$P<0.005$
HDAC3-Hs00187320_m1	41.3957745	$P<0.05$
CASP3-Hs00234387_m1	41.39331585	$P<0.005$
JMJD4-Hs01061169_m1	41.29007126	$P<0.0005$
GSK3B-Hs00275656_m1	40.34632151	$P<0.05$
GTF2B-Hs00155321_m1	40.19048896	$P<0.005$
HDAC4-Hs00195814_m1	40.10003337	$P<0.05$
PSMB2-Hs01002946_m1	40.03032093	$P<0.005$
CBFB-Hs00242387_m1	40.01894293	$P<0.05$
CASP9-Hs00154260_m1	39.6212818	$P<0.005$
GAPDH-Hs99999905_m1	39.45539253	$P<0.005$
VEGFB-Hs00173634_m1	38.55567983	$P<0.005$
GATA3-Hs00231122_m1	38.41059059	$P<0.005$
MAPK14-Hs00176247_m1	38.05872744	$P<0.05$
PSMC2-Hs00739800_m1	38.0290858	$P<0.005$
MAPK3-Hs00385075_m1	37.51114806	$P<0.005$
CACNB4-Hs00167878_m1	37.16357932	$P<0.005$
INPP5D-Hs00183290_m1	37.14258136	$P<0.005$
GRB2-Hs00157817_m1	36.9891534	$P<0.05$
PSMB5-Hs00605652_m1	36.97894053	$P<0.05$
RB1-Hs01078066_m1	36.90756433	$P<0.0005$
ABL1;BCR-Hs00245445_m1	36.81411873	$P<0.05$
VDR-Hs01045840_m1	36.32582263	$P<0.005$
RAF1-Hs00234119_m1	36.14930246	$P<0.005$
SIRT1-Hs01009006_m1	35.85850486	$P<0.005$
HDAC8-Hs00218503_m1	35.85287274	$P<0.005$
PRKCD-Hs01090047_m1	35.35934633	$P<0.005$
PLCB1-Hs00248563_m1	35.28520599	$P<0.05$
COL19A1-Hs00156940_m1	35.24923961	$P<0.005$
PSMC3-Hs00267682_m1	34.76949247	$P<0.05$
PSMC4-Hs00197826_m1	34.75465601	$P<0.05$
PRKAR1B-Hs00406762_m1	34.54533798	$P<0.05$
DDR1-Hs00233612_m1	34.38126556	$P<0.005$
ITPR1-Hs00181881_m1	34.34596481	$P<0.005$

(*Contd*...)

Table 2: Continued

(*Contd*...)

Table 2: Continued

Twin os (n=2) vs non-os (n=4)		
Gene	**R/Q**	**BH (56%)**
GADD45G-Hs00198672_m1	34.26597171	$P<0.05$
TAB1-Hs00196143_m1	34.16783805	$P<0.0005$
PIK3CA-Hs00180679_m1	33.87132397	$P<0.005$
ATR-Hs00354807_m1	33.82496736	$P<0.05$
EP300-Hs00230938_m1	33.80868932	$P<0.005$
ACVR2B-Hs00609603_m1	33.4621255	$P<0.05$
CASP2-Hs00234982_m1	32.85577281	$P<0.05$
PTEN-Hs01920652_s1	32.81195837	$P<0.005$
PRKACB-Hs00176944_m1	32.81096995	$P<0.005$
PRKCE-Hs00178455_m1	32.62503402	$P<0.0005$
CDK4-Hs00175935_m1	32.55518355	$P<0.005$
DVL2-Hs00182901_m1	32.43859181	$P<0.005$
CAMK2D-Hs00241833_m1	32.35887661	$P<0.05$
TAB2-Hs00248373_m1	32.35869844	$P<0.05$
MAPK1-Hs01046830_m1	32.26353183	$P<0.05$
PRKDC-Hs00179161_m1	32.20590998	$P<0.005$
TFRC-Hs99999911_m1	32.0255323	$P<0.005$
BCL2-Hs99999018_m1	31.98634237	$P<0.0005$
SMAD4-Hs00929647_m1	31.75346606	$P<0.005$
EFNB1-Hs00270004_m1	31.69950049	$P<0.005$
PIAS1-Hs00184008_m1	31.59519581	$P<0.005$
MAP2K4-Hs00387426_m1	31.10665912	$P<0.05$
ELK1-Hs00428286_g1	31.01493418	$P<0.005$
PRKCB-Hs00176998_m1	30.86544478	$P<0.005$
E2F6-Hs00242501_m1	30.83945104	$P<0.005$
CACNB1-Hs00609501_m1	30.59402173	$P<0.05$
ATM-Hs01112307_m1	30.48818951	$P<0.005$
SIRT2-Hs00247263_m1	30.43753762	$P<0.005$
PSMC5-Hs00267687_m1	30.12796121	$P<0.0005$
HDAC10-Hs00368899_m1	29.7331829	$P<0.05$
MDM2-Hs99999008_m1	29.45532391	$P<0.005$
MAP3K7-Hs00177373_m1	29.38079948	$P<0.005$
SMAD3-Hs00232222_m1	29.23583914	$P<0.005$
CREB1-Hs00231713_m1	28.88115729	$P<0.05$
PUM1-Hs00206469_m1	28.77393578	$P<0.005$
HDAC5-Hs00608366_m1	28.73987704	$P<0.005$
CASP1-Hs00354836_m1	28.63819756	$P<0.05$
ATF2-Hs00153179_m1	28.54531252	$P<0.005$
CREB3L4-Hs00370116_m1	28.4467662	$P<0.005$
CASP10-Hs01017902_m1	28.41388429	$P<0.05$
TP53-Hs01034249_m1	28.16113504	$P<0.005$
PRKAR2A-Hs00177760_m1	27.53676717	$P<0.05$
EIF2B1-Hs00426752_m1	27.46093807	$P<0.05$
HPRT1-Hs99999909_m1	27.17679034	$P<0.05$
HIPK2-Hs00179759_m1	27.05025347	$P<0.005$
LTBP3-Hs00221445_m1	26.83850085	$P<0.005$
HDAC2-Hs00231032_m1	26.78680935	$P<0.05$
PSMA2-Hs00855061_sH	26.63525188	$P<0.05$
BAX-Hs00180269_m1	26.15599313	$P<0.005$

(*Contd*...)

Table 2: Continued

Twin os (n=2) vs non-os (n=4)		
Gene	**R/Q**	**BH (56%)**
CDK2-Hs01548894_m1	26.13292739	$P<0.005$
SATB1-Hs00161515_m1	26.03928831	$P<0.005$
PSMA6-Hs00853240_sH	26.02093338	$P<0.005$
SMAD4-Hs00232068_m1	25.83323033	$P<0.005$
CALM1-Hs00237233_m1	25.77014659	$P<0.005$
GNB1-Hs00181845_m1	24.69083394	$P<0.005$
BMPR2-Hs00176148_m1	24.62245822	$P<0.005$
ABL1-Hs01104728_m1	24.61795195	$P<0.005$
PSMD4-Hs00356654_m1	24.57953187	$P<0.005$
TNFRSF10B-Hs00366278_m1	24.12849866	$P<0.05$
PPIA-Hs99999904_m1	23.92599791	$P<0.05$
AKT2-Hs01086102_m1	23.92056217	$P<0.005$
AKT3-Hs00178533_m1	23.90283245	$P<0.005$
PIK3R1-Hs00381459_m1	23.84109847	$P<0.005$
SIRT3-Hs00202030_m1	23.54284675	$P<0.005$
HDAC9-Hs00206843_m1	23.23657342	$P<0.05$
TGFB1-Hs00998133_m1	23.21367265	$P<0.005$
SMAD2-Hs00183425_m1	22.83644723	$P<0.005$
CHEK1-Hs00967506_m1	22.83572474	$P<0.05$
HDAC7-Hs00248789_m1	22.62838313	$P<0.005$
ATF1-Hs00270896_m1	22.09395959	$P<0.005$
GUSB-Hs99999908_m1	21.8421666	$P<0.05$
RELB-Hs00232399_m1	21.80654839	$P<0.05$
BRCA1-Hs01556193_m1	21.74461398	$P<0.005$
POLR2A-Hs00172187_m1	21.44807146	$P<0.005$
RPS17-Hs00734303_g1	21.0322051	$P<0.05$
CALM3-Hs00270914_m1	20.18818718	$P<0.005$
HOXA1-Hs00939046_m1	19.94715129	$P<0.05$
MAP2K6-Hs00992389_m1	19.93605922	$P<0.05$
JUN-Hs99999141_s1	19.67108465	$P<0.005$
CREM-Hs01582003_g1	19.59083741	$P<0.005$
SMAD6-Hs00178579_m1	18.90720269	$P<0.05$
TGFB1-Hs99999918_m1	18.78369714	$P<0.005$
PRKACG-Hs01033925_s1	18.11711499	$P<0.05$
CCNE1-Hs01026536_m1	17.88807742	$P<0.05$
PRKCA-Hs00176973_m1	17.55625604	$P<0.05$
COL1A1-Hs00164004_m1	17.36127983	$P<0.005$
MSX2-Hs00751239_s1	16.76995145	$P<0.005$
PES1-Hs00362795_g1	16.74832062	$P<0.05$
BMPR1A-Hs01034913_g1	16.64656557	$P<0.005$
RPL30-Hs00265497_m1	15.71607734	$P<0.05$
E2F4-Hs00608098_m1	15.29984765	$P<0.005$
CDKN1A-Hs00355782_m1	15.15061788	$P<0.05$
HDAC1-Hs02621185_s1	15.11899763	$P<0.005$
FGF2-Hs00266645_m1	14.90047621	$P<0.005$
CASC3-Hs00201226_m1	14.54674123	$P<0.005$
BAI1-Hs00181777_m1	14.0180953	$P<0.05$
BMPR1A-Hs00831730_s1	13.98018185	$P<0.005$

(*Contd*...)

Table 2: Continued

Twin os (n=2) vs non-os (n=4)		
Gene	**R/Q**	**BH (56%)**
EIF4E-Hs00908915_g1	13.9589797	$P<0.05$
BMP6-Hs00233470_m1	13.35696978	$P<0.005$
IHH-Hs00745531_s1	13.26092052	$P<0.05$
ACVR1-Hs00153836_m1	13.00447825	$P<0.005$
CHEK2-Hs00200485_m1	12.92288988	$P<0.005$
CACNB3-Hs00167873_m1	12.67721395	$P<0.05$
HDAC6-Hs00195869_m1	12.52217699	$P<0.005$
COL4A4-Hs00164150_m1	11.96933439	$P<0.005$
GNB2-Hs00929275_g1	11.79646015	$P<0.05$
ADCY3-Hs00269618_m1	11.54764087	$P<0.05$
KAT2B-Hs00187332_m1	10.6524953	$P<0.05$
OAZ1-Hs00427923_m1	10.36895925	$P<0.05$
GNAS-Hs00255603_m1	9.843423704	$P<0.05$
PDGFA-Hs00234994_m1	9.287349766	$P<0.05$
PIK3R2-Hs00178181_m1	8.060432114	$P<0.05$
TNNT1-Hs00162848_m1	8.050441173	$P<0.05$
E2F1-Hs00153451_m1	7.929855963	$P<0.05$
ATF4-Hs00909568_g1	7.697303147	$P<0.05$
PRKAR2B-Hs00176966_m1	6.308900397	$P<0.05$

BH: Benjamini-Hochberg correction, RQ: Relative quantification value

MMP8 was increased 95-fold in Os patients (P = ns); this gene is located on chromosome 11q22.3 and encodes a matrix metalloproteinase that is stored in neutrophil granules and functions in the degradation of collagen types I, II and III. KIT was elevated 58-fold in the Os patients (P = ns). HIF1A was elevated 43-fold in the Os group. This gene is located on chromosome 14q23.2 and encodes the alpha subunit of hypoxia-inducible factor-1, a transcription factor, which functions in cellular homeostasis in response to hypoxia. CREB3 was elevated 41-fold in the Os group; this gene is located on chromosome 9p13.3 and encodes a transcription factor that regulates cell proliferation. CREB3 is involved in establishing latent herpes simplex virus infections and also plays a role in leukocyte migration, tumor suppression, and endoplasmic reticulum stress-associated protein degradation. YWHAZ was elevated 36-fold in the os patients (P = ns); this gene is located on chromosome 8q23.1 and belongs to the 14-3-3 family of proteins. It is involved in signal transduction and has been shown to interact with the insulin receptor-substrate-1 protein. TGFBR1 was elevated 32-fold in os patients (P = ns); it is located on chromosome 9q22 and encodes a Ser/Thr protein kinase involved in signal transduction. NFKB2 was elevated 27-fold in the os group. The gene is located on chromosome 10q24 and encodes the beta-subunit of the NF-kB transcription factor complex, which serves to activate inflammatory responses. FGFR1 was elevated 25-fold (P = ns) in the os patients. This gene is located on 8p12 and encodes a tyrosine-kinase protein that binds both basic and acidic fibroblast growth factor and mediates cell differentiation and mitogenesis. Mutations in this gene are associated with Pfeiffer syndrome, Jackson–Weiss syndrome, Antley–Bixler syndrome, osteoglophonic dysphagia, and autosomal dominant Kallman syndrome 2. IPO8 was increased 25-fold; this gene is located on chromosome 12p11.21 and encodes a protein that modulates Ran GTPase activity. STAT1 was increased 24-fold; this gene is located on chromosome 2q32.2 and encodes a protein that serves as a transcription activator in response to cytokine and growth factor signaling. In addition to the 10 genes reported above, COL1A1 was found to be elevated 14.8-fold (P = ns) and BMP3 was elevated 6.6-fold (P = ns) in the Os group. The COL1A1 gene is located on chromosome 17q21.23 and encodes the pro-alpha1 chain of type-1 collagen, which is found in most connective tissues and is abundant in bone. Mutations in COL1A1 are associated with osteogenesis imperfect types I-IV, Ehlers–Danlos syndrome type VIIA, Ehlers–Danlos syndrome Classical type, Caffey disease and idiopathic osteoporosis. BMP3 (osteogenin) is a gene that is located on chromosome 4q21 and encodes a member of the TGF-B superfamily that induces bone formation.

DISCUSSION

The identification of a pair of identical twins without a history of trauma both harboring os odontoidea of nearly identical morphology [Figures 1 and 2] lends further support to the concept of a congenital etiology for this disorder at least for some individuals. While the traumatic hypothesis has been widely supported, it is clear from this and other studies[7,18,19,33,42] that the development an os odontoideum may result from a different process. Some cases may be clearly traumatic in origin and as such represent odontoid fracture nonunions, others have a congenital etiology and there may be a few that represent a combination of the two.

Numerous case reports and case series attest to the rarity of this anomaly and neither the overall incidence nor the prevalence is well documented. The closest (albeit flawed) estimate is provided by Sankar *et al.*,[33] who noted a 3.1% prevalence of os odontoideum following a review of all abnormal radiographs at the Children's Hospital of Philadelphia. In this series of 16 patients, only 3 individuals were identified as having a clinical history compatible with a traumatic etiology, while 6 harbored associated cervical spine anomalies. If one accepts the existence of both a traumatic and congenital etiology,[33] the question of whether these two separate etiologies result in distinct clinical disorders, especially with regards to ligamentous competency and overall spinal stability must be addressed as this may impact the natural history and accordingly treatment recommendations.

Table 3: Twins vs non-twin os

Twin os (n=2) vs non-twin os (n=2)				
Gene	**R/Q**	**BH**	**Location**	**NCBI Gene summary[28]**
CAMK4	31.22	$P<0.05$	5q21.3	The product of this gene belongs to the serine/threonine protein kinase family, and to the Ca (2+)/calmodulin-dependent protein kinase subfamily. This enzyme is a multifunctional serine/threonine protein kinase with limited tissue distribution, which has been implicated in transcriptional regulation in lymphocytes, neurons and male germ cells
ATF1	23.04	$P<0.05$	12q. 13	This gene encodes an activating transcription factor, which belongs to the ATF subfamily and bZIP (basic-region leucine zipper) family. It influences cellular physiologic processes by regulating the expression of downstream target genes, which are related to growth, survival, and other cellular activities. This protein is phosphorylated at serine 63 in its kinase-inducible domain by serine/threonine kinases, cAMP-dependent protein kinase A, calmodulin-dependent protein kinase I/II, mitogen- and stress-activated protein kinase and cyclin-dependent kinase 3 (cdk-3). Its phosphorylation enhances its transactivation and transcriptional activities, and enhances cell transformation. Fusion of this gene and FUS on chromosome 16 or EWSR1 on chromosome 22 induced by translocation generates chimeric proteins in angiomatoid fibrous histiocytoma and clear cell sarcoma. This gene has a pseudogene on chromosome 6
PLCG1	21.22	$P<0.05$	20q12-q13.1	The protein encoded by this gene catalyzes the formation of inositol 1,4,5-trisphosphate and diacylglycerol from phosphatidylinositol 4,5-bisphosphate. This reaction uses calcium as a cofactor and plays an important role in the intracellular transduction of receptor-mediated tyrosine kinase activators. For example, when activated by SRC, the encoded protein causes the Ras guanine nucleotide exchange factor RasGRP1 to translocate to the Golgi, where it activates Ras. Also, this protein has been shown to be a major substrate for heparin-binding growth factor 1 (acidic fibroblast growth factor)-activated tyrosine kinase. Two transcript variants encoding different isoforms have been found for this gene
TAB1	20.65	$P<0.05$	22q13.1	The protein encoded by this gene was identified as a regulator of the MAP kinase kinase kinase MAP3K7/TAK1, which is known to mediate various intracellular signaling pathways, such as those induced by TGFB, interleukin 1, and WNT-1. This protein interacts and thus activates TAK1 kinase. It has been shown that the C-terminal portion of this protein is sufficient for binding and activation of TAK1, while a portion of the N-terminus acts as a dominant-negative inhibitor of TGF beta, suggesting that this protein may function as a mediator between TGF beta receptors and TAK1. This protein can also interact with and activate the mitogen-activated protein kinase 14 (MAPK14/p38alpha), and thus represents an alternative activation pathway, in addition to the MAPKK pathways, which contributes to the biological responses of MAPK14 to various stimuli. Alternatively spliced transcript variants encoding distinct isoforms have been reported
E2F3	18.63	$P<0.05$	6p22	The protein encoded by this gene is a member of the E2F family of transcription factors. The E2F family plays a crucial role in the control of cell cycle and action of tumor suppressor proteins and is also a target of the transforming proteins of small DNA tumor viruses. The E2F proteins contain several evolutionally conserved domains found in most members of the family. These domains include a DNA binding domain, a dimerization domain which determines interaction with the differentiation regulated transcription factor proteins (DP), a transactivation domain enriched in acidic amino acids, and a tumor suppressor protein association domain, which is embedded within the transactivation domain. This protein and another 2 members, E2F1 and E2F2, have an additional cyclin binding domain. This protein binds specifically to retinoblastoma protein pRB in a cell-cycle dependent manner. Two transcript variants encoding different isoforms have been found for this gene
ATF4	13.93	$P<0.05$	22q13.1	This gene encodes a transcription factor that was originally identified as a widely expressed mammalian DNA binding protein that could bind a tax-responsive enhancer element in the LTR of HTLV-1. The encoded protein was also isolated and characterized as the cAMP-response element binding protein 2 (CREB-2). The protein encoded by this gene belongs to a family of DNA-binding proteins that includes the AP-1 family of transcription factors, cAMP-response element binding proteins and CREB-like proteins. These transcription factors share a leucine zipper region that is involved in protein–protein interactions, located C-terminal to a stretch of basic amino acids that functions as a DNA binding domain. Two alternative transcripts encoding the same protein have been described. Two pseudogenes are located on the X chromosome at q28 in a region containing a large inverted duplication

CREB-2: cAMP-response element binding protein 2, BH: Benjamini-Hochberg correction, RQ: Relative quantification value

This study identified a litany of significant differences in gene expression (213/380 genes in total) between the Twins with the non-os group. Notably, these genes have biological functionality related to bone formation and maintenance. PHEX, a gene involved in bone mineralization, was elevated 447-fold in the Twins. TUFT1, another gene related to mineralization (of enamel), was increased 109-fold. TFGBI, a gene that mediates cell–collagen interactions and is thought to be involved in endochondral bone formation, was elevated 92-fold. MMP8, a neutrophil MMP that breaks down collagen types I, II, and III, was elevated 90-fold

Table 4: Top 10 RQ values in os vs non-os with uncorrected $P<0.1$

Os ($n=4$) vs non-os ($n=4$)				
Gene	**R/Q**	**BH**	**Location**	**NCBI Gene summary[28]**
MMP8	95.31	$P=$ns	11q22.3	Proteins of the matrix metalloproteinase family are involved in the breakdown of extracellular matrix in normal physiological processes, such as embryonic development, reproduction, and tissue remodeling, as well as in disease processes, such as arthritis and metastasis. Most MMPs are secreted as inactive proproteins, which are activated when cleaved by extracellular proteinases. However, the enzyme encoded by this gene is stored in secondary granules within neutrophils and is activated by autolytic cleavage. Its function is degradation of type I, II, and III collagens. The gene is part of a cluster of MMP genes, which localize to chromosome 11q22.3
KIT	58.47	$P=$ns	4q11-q12	This gene encodes the human homolog of the proto-oncogene c-kit. C-kit was first identified as the cellular homolog of the feline sarcoma viral oncogene v-kit. This protein is a type 3 transmembrane receptor for MGF (mast cell growth factor, also known as stem cell factor). Mutations in this gene are associated with gastrointestinal stromal tumors, mast cell disease, acute myelogenous leukemia, and piebaldism. Multiple transcript variants encoding different isoforms have been found for this gene
HIF1A	42.76	$P=$ns	14q23.2	This gene encodes the alpha subunit of transcription factor hypoxia-inducible factor-1 (HIF-1), which is a heterodimer composed of an alpha and a beta subunit. HIF-1 functions as a master regulator of cellular and systemic homeostatic response to hypoxia by activating transcription of many genes, including those involved in energy metabolism, angiogenesis, apoptosis, and other genes whose protein products increase oxygen delivery or facilitate metabolic adaptation to hypoxia. HIF-1 thus plays an essential role in embryonic vascularization, tumor angiogenesis and pathophysiology of ischemic disease. Alternatively spliced transcript variants encoding different isoforms have been identified for this gene
CREB3	41.37	$P=$ns	9p13.3	This gene encodes a transcription factor that is a member of the leucine zipper family of DNA binding proteins. This protein binds to the cAMP-response element and regulates cell proliferation. The protein interacts with host cell factor C1, which also associates with the herpes simplex virus (HSV) protein VP16 that induces transcription of HSV immediate-early genes. This protein and VP16 both bind to the same site on host cell factor C1. It is thought that the interaction between this protein and host cell factor C1 plays a role in the establishment of latency during HSV infection. This protein also plays a role in leukocyte migration, tumor suppression, and endoplasmic reticulum stress-associated protein degradation. Additional transcript variants have been identified, but their biological validity has not been determined
YWHAZ	36.39	$P=$ns	8q23.1	This gene product belongs to the 14-3-3 family of proteins, which mediate signal transduction by binding to phosphoserine-containing proteins. This highly conserved protein family is found in both plants and mammals, and this protein is 99% identical to the mouse, rat and sheep orthologs. The encoded protein interacts with IRS1 protein, suggesting a role in regulating insulin sensitivity. Several transcript variants that differ in the 5′ UTR but that encode the same protein have been identified for this gene
TGFBR1	31.67	$P=$ns	9q22	The protein encoded by this gene forms a heteromeric complex with type II TGF-beta receptors when bound to TGF-beta, transducing the TGF-beta signal from the cell surface to the cytoplasm. The encoded protein is a serine/threonine protein kinase. Mutations in this gene have been associated with Loeys-Dietz aortic aneurysm syndrome. Multiple transcript variants encoding different isoforms have been found for this gene
NFKB2	26.72	$P=$ns	10q24	This gene encodes one of the subunits of the transcription factor complex nuclear factor-kappa-B (NFkB). The NFkB transcription factor complex is expressed in numerous cell types and functions as a central activator of genes involved in inflammation and immune function. The NFkB complex can consist of different subunits that form both homo- or heterodimers which bind specific kappa-B elements in target genes. This gene encodes the p100 subunit that is processed into the active p52 subunit. This protein can function as both a transcriptional activator and repressor, depending on its dimer partner. Alternate splicing results in both coding and noncoding variants
FGFR1	25.39	$P=$ns	8p12	The protein encoded by this gene is a member of the fibroblast growth factor receptor family, where amino acid sequence is highly conserved between members and throughout evolution. FGFR family members differ from one another in their ligand affinities and tissue distribution. A full-length representative protein consists of an extracellular region, composed of three immunoglobulin-like domains, a single hydrophobic membrane-spanning segment and a cytoplasmic tyrosine kinase domain. The extracellular portion of the protein interacts with fibroblast growth factors, setting in motion a cascade of downstream signals, ultimately influencing mitogenesis and differentiation. This particular family member binds both acidic and basic fibroblast growth factors and is involved in limb induction. Mutations in this gene have been associated with Pfeiffer syndrome, Jackson-Weiss syndrome, Antley-Bixler syndrome, osteoglophonic dysplasia, and autosomal dominant Kallmann syndrome 2. Chromosomal aberrations involving this gene are associated with stem cell myeloproliferative disorder and stem cell leukemia lymphoma syndrome. Alternatively spliced variants which encode different protein isoforms have been described; however, not all variants have been fully characterized

(*Contd*...)

Table 4: Top 10 RQ values in os vs non-os with uncorrected $P<0.1$

Os ($n=4$) vs non-os ($n=4$)				
Gene	**R/Q**	**BH**	**Location**	**NCBI Gene summary[28]**
IPO8	24.75	$P=$ns	12p11.21	The importin-alpha/beta complex and the GTPase Ran mediate nuclear import of proteins with a classical nuclear localization signal. The protein encoded by this gene is a member of a class of approximately 20 potential Ran targets that share a sequence motif related to the Ran-binding site of importin-beta. This protein binds to the nuclear pore complex and, along with RanGTP and RANBP1, inhibits the GAP stimulation of the Ran GTPase. Alternatively spliced transcript variants encoding different isoforms have been found for this gene
STAT1	23.81	$P=$ns	2q32.2	The protein encoded by this gene is a member of the STAT protein family. In response to cytokines and growth factors, STAT family members are phosphorylated by the receptor associated kinases, and then form homo- or heterodimers that translocate to the cell nucleus where they act as transcription activators. This protein can be activated by various ligands including interferon-alpha, interferon-gamma, EGF, PDGF, and IL6. This protein mediates the expression of a variety of genes, which is thought to be important for cell viability in response to different cell stimuli and pathogens. Two alternatively spliced transcript variants encoding distinct isoforms have been described
COL1A1	14.83	$P=$ns	17q21.23	This gene encodes the pro-alpha1 chains of type I collagen whose triple helix comprises two alpha1 chains and one alpha2 chain. Type I is a fibril-forming collagen found in most connective tissues and is abundant in bone, cornea, dermis and tendon. Mutations in this gene are associated with osteogenesis imperfecta types I-IV, Ehlers-Danlos syndrome type VIIA, Ehlers–Danlos syndrome Classical type, Caffey Disease and idiopathic osteoporosis. Reciprocal translocations between chromosomes 17 and 22, where this gene and the gene for platelet-derived growth factor beta are located, are associated with a particular type of skin tumor called dermatofibrosarcoma protuberans, resulting from unregulated expression of the growth factor. Two transcripts, resulting from the use of alternate polyadenylation signals, have been identified for this gene
BMP3	6.63	$P=$ns	4q21	BMP3 belongs to the TGFB superfamily. Bone morphogenic protein, also known as osteogenin, induces bone formation

MMP: Matrix metalloproteinase, FGFR: Fibroblast growth factor receptor LDAS: Loeys-Dietz aortic aneurysm syndrome, TGFB: Transforming growth factor beta, BH: Benjamini-Hochberg correction, RQ: Relative quantification value

in the Twins. RUNX2, encodes a transcription factor that induces osteoblastic differentiation and is critical in skeletal morphogenesis, was elevated 66-fold in the Twins. Though none of the expression profiles comparing the os patients to the non-os subjects held statistical significance, we found trends in genes similarly involved in bone development and maintenance. MMP8 again was elevated 95-fold; FGFR1 was elevated 25-fold; COL1A1 was elevated 15-fold and BMP3 was elevated 7-fold. Further investigation of these genes may aid in further understanding of the cellular and molecular pathogenesis of os odontoideum.

This study is compromised by the small sample size, which may, in part, be responsible for the lack of statistical significance in the trends in gene expression profile that we found between the os and non-os groups. We opted to include the gene expression profile from the Twins' mother in order to control for potential hereditary gene expression patterns unrelated to os odontoideum. The comparison group does not contain age-matched cases, adding a potential confounding variable. There is also the limitation of data selection: There were over 200 genes with significant differences in expression profiles between the Twins and the non-os controls. The strategy employed to overcome this potential problem was to focus on those genes with the greatest magnitude of change. Though this approach allows for a concise and informative presentation of the results, it may have excluded some relevant gene profiles.

CONCLUSION

Os odontoideum has multiple etiologies, both congenital and traumatic and perhaps some cases represent a combination of the two. Further definition of each type and examination of their relative prevalence will be informative. Moreover, investigation of the relevance of this distinction as to the clinical evaluation, natural history, and treatment is appropriate. We have identified a number of genes that show increased expression in a pair of twins with congenital os odontoideum and also demonstrated trends in gene expression profiles between a larger group of os odontoideum patients and non-os patients. A number of these genes are related to bone morphogenesis and maintenance. Further investigations of the molecular biology of these genes may confer a greater understanding of this anomaly.

REFERENCES

1. Al Kaissi A, Chehida FB, Ghachem MB, Grill F, Klaushofer K. Atlanto-axial segmentation defects and os odontoideum in two male siblings with

opsismodysplasia. Skeletal Radiol 2009;38:293-6.
2. Arvin B, Fournier-Gosselin MP, Fehlings MG. Os odontoideum: Etiology and surgical management. Neurosurgery 2010;66 (3 Suppl):22-31.
3. Asagiri M, Takayanagi H. The molecular understanding of osteoclast differentiation. Bone 2007;40:251-64.
4. Benjamini Y, Hochberg Y. Controlling the false discovery rate: A practical and powerful approach to multiple testing. J R Stat Soc B 1995;57:289-300.
5. Brazma A, Hingamp P, Quackenbush J, Sherlock G, Spellman P, Stoeckert C, *et al*. Minimum information about a microarray experiment (MIAME)-toward standards for microarray data. Nat Genet 2001;29:365-72.
6. Clements WD, Mezue W, Mathew B. Os odontoideum--congenital or acquired?--that's not the question. Injury 1995;26:640-2.
7. Currarino G. Segmentation defect in the midodontoid process and its possible relationship to the congenital type of os odontoideum. Pediatr Radiol 2002;32:34-40.
8. Ellies DL, Krumlauf R. Bone formation: The nuclear matrix reloaded. Cell 2006;125:840-2.
9. Fagan AB, Askin GN, Earwaker JW. The jigsaw sign. A reliable indicator of congenital aetiology in os odontoideum. Eur Spine J 2004;13:295-300.
10. Fielding JW, Griffin PP. Os odontoideum: An acquired lesion. J Bone Joint Surg Am 1974;56:187-90.
11. Fielding JW, Hensinger RN, Hawkins RJ. Os Odontoideum. J Bone Joint Surg Am 1980;62:376-83.
12. Freiberger RH, Wilsonjr PD, Nicholas JA. Acquired Absence of the Odontoid Process A case report. J Bone Joint Surg Am 1965;47:1231-6.
13. Gadgil M, Lian W, Gadgil C, Kapur V, Hu WS. An analysis of the use of genomic DNA as a universal reference in two channel DNA microarrays. BMC Genomics 2005;6:66.
14. Garcion C, Baltensperger R, Fournier T, Pasquier J, Schnetzer MA, Gabriel JP, *et al*. FiRe and microarrays: A fast answer to burning questions. Trends Plant Sci 2006;11:320-2.
15. Hadley, MN. Os odontoideum. Neurosurgery 2002;50:S148-55.
16. Hawkins RJ, Fielding JW, Thompson WJ. Os odontoideum: Congenital or acquired. A case report. J Bone Joint Surg Am 1976;58:413-4.
17. Karsenty G, Kronenberg HM, Settembre C. Genetic control of bone formation. Annu Rev Cell Dev Biol 2009;25:629-48.
18. Kirlew KA, Hathout GM, Reiter SD, Gold RH. Os odontoideum in identical twins: Perspectives on etiology. Skeletal radiology 1993;22:525-7.
19. Klimo *P* Jr, Coon V, Brockmeyer D. Incidental os odontoideum: Current management strategies. Neurosurg Focus 2011;31:E10.
20. Klimo *P* Jr, Kan P, Rao G, Apfelbaum R, Brockmeyer D. Os odontoideum: Presentation, diagnosis, and treatment in a series of 78 patients. J Neurosurg Spine 2008;9:332-42.
21. Kovacs B, Lumayag S, Cowan C, Xu S. MicroRNAs in early diabetic retinopathy in streptozotocin-induced diabetic rats. Invest Ophthalmol Vis Sci 2011;52:4402-9.
22. Lian JB, Stein GS, Javed A, van Wijnen AJ, Stein JL, Montecino M, *et al*. Networks and hubs for the transcriptional control of osteoblastogenesis. Rev Endocr Metab Disord 2006;7:1-16.
23. Mao Z, Shay B, Hekmati M, Fermon E, Taylor A, Dafni L, *et al*. The human tuftelin gene: cloning and characterization. Gene 2001;279:181-96.
24. McCarthy JG, Stelnicki EJ, Mehrara BJ, Longaker MT. Distraction osteogenesis of the craniofacial skeleton. Plast Reconstr Surg 2001;107:1812-27.
25. Menezes AH. Pathogenesis, dynamics, and management of os odontoideum. Neurosurg Focus 1999;6:e2.
26. Morgan MK, Onofrio BM, Bender CE. Familial os odontoideum. Case report. J Neurosurg 1989;70:636-9.
27. Morriss-Kay GM, Wilkie AO. Growth of the normal skull vault and its alteration in craniosynostosis: Insights from human genetics and experimental studies. J Anat 2005;207:637-53.
28. NCBI. NCBI Gene. Available from: http://www.ncbi.nlm.nih.gov/gene. [Last accessed on 2012 Oct 12].
29. Peeters JK, Van der Spek PJ. Growing applications and advancements in microarray technology and analysis tools. Cell Biochem Biophys 2005;43:149-66.
30. Provot S, Schipani E. Molecular mechanisms of endochondral bone development. Biochem Biophys Res Commun 2005;328:658-65.
31. Ricciardi JE, Kaufer H, Louis DS. Acquired os odontoideum following acute ligament injury. Report of a case. J Bone Joint Surg Am 1976;58:410-2.
32. Rieu I, Powers SJ. Real-time quantitative RT-PCR: Design, calculations, and statistics. Plant Cell 2009;21:1031-3.
33. Sankar WN, Wills BPD, Dormans JP, Drummond DS. Os odontoideum revisited: The case for a multifactorial etiology. Spine (Phila Pa 1976) 2006;31:979-84.
34. Schmitt JM, Hwang K, Winn SR, Hollinger JO. Bone morphogenetic proteins: An update on basic biology and clinical relevance. J Orthop Res 1999;17:269-78.
35. Schuler TC, Kurz L, Thompson DE, Zemenick G, Hensinger RN, Herkowitz HN. Natural history of os odontoideum. J Pediatr Orthop 1991;11:222-5.
36. Stains JP, Civitelli R. Cell-to-cell interactions in bone. Biochem Biophys Res Commun 2005;328:721-7.
37. Stillwell WT, Fielding JW. Acquired os odontoideum. A case report. Clin Orthop Relat Res 1978;135:71-3.
38. Teitelbaum SL, Ross FP. Genetic regulation of osteoclast development and function. Nat Rev Genet 2003;4:638-49.
39. Tsiridis E, Giannoudis PV. Transcriptomics and proteomics: Advancing the understanding of genetic basis of fracture healing. Injury 2006;37 Suppl 1:S13-9.
40. Verska JM, Anderson PA. Os odontoideum. A case report of one identical twin. Spine 1997;22:706-9.
41. Wan M, Cao X. BMP signaling in skeletal development. Biochem Biophys Res Commun 2005;328:651-7.
42. Wang S, Wang C. Acquired os odontoideum: A case report and literature review. Childs Nerv Syst 2012;28:315-9.
43. Wang S, Wang C. Familial dystopic os odontoideum: A report of three cases. J Bone Joint Surg Am 2011;93:e44.
44. Weston AD, Ozolins TR, Brown NA. Thoracic skeletal defects and cardiac malformations: A common epigenetic link? Birth Defects Res C Embryo Today 2006;78:354-70.
45. Yamamoto T, Kurosawa K, Masuno M, Okuzumi S, Kondo S, Miyama S, *et al*. Congenital anomaly of cervical vertebrae is a major complication of Rubinstein-Taybi syndrome. Am J Med Genet A 2005;135:130-3.
46. Yuan JS, Reed A, Chen F, Stewart CN Jr. Statistical analysis of real-time PCR data. BMC Bioinformatics 2006;7:85.
47. Zaidi M, Brain SD, Tippins JR, Di Marzo V, Moonga BS, Chambers TJ, *et al*. Structure-activity relationship of human calcitonin-gene-related peptide. Biochem J 1990;269:775-80.
48. Zygourakis CC, Cahill KS, Proctor MR. Delayed development of os odontoideum after traumatic cervical injury: Support for a vascular etiology. J Neurosurg Pediatr 2011;7:201-4.